Technology and Health Care 7 (1999) 243–259
IOS Press

Dynamic delay time compensation for sampling capillaries used in respiratory mass spectrometry

Luc Eberhard [a], Christoph Haberthür [a], Ben Fabry [b] and Josef Guttmann [c]

[a] *Department of Internal Medicine, University Clinics Basel, Spitalstrasse 21, CH-4031 Basel, Switzerland*

[b] *Physiology Program, Harvard School of Public Health, 665 Huntington Av, Boston, MA 02115, USA*

[c] *Institute of Experimental Anesthesiology, University Clinics of Anesthesiology, Hugstetterstrasse 55, D-79106 Freiburg, Germany*

Received in final form 3 November 1998

Abstract. In intensive care patients who receive ventilatory support or full mechanical ventilation, valuable information can be drawn from gas exchange measurements. In this setting, the most favorable method for gas exchange measurement is by simultaneous recording of gas concentrations and gas flow, and by time resolved multiplication and accumulation. This paper presents a new method to compensate for the signal delay time which occurs when a sampling capillary is used for measuring gas concentrations with a respiratory mass spectrometer or some equivalent sidestream gas analyzer. The signal delay of gas concentrations must be accurately compensated to avoid error accumulation in gas exchange calculation. A delay time can be easily measured with a test gas in a laboratory setup and be readily compensated for during the measurements in a ventilated patient. This is a standard procedure which gives reasonable results under normal conditions. Special attention is however required in cases where the gas viscosity changes due to large changes in gas composition, e.g., those used for diagnostic breathing or ventilatory maneuvers. Such changes of viscosity will influence the delay time of the capillary, because they affect its flow resistance. As a consequence they will degrade the quality of measurements when done with a simple fixed delay compensation. The method described here consists of an algorithm which enables compensation for such a temporally changing delay time due to changes in gas composition.

Keywords: ICU patient, ventilatory support, gas exchange, FRC, mass spectrometry, sampling capillary, gas transport, gas viscosity, delay time

1. Introduction

There exists a variety of standard methods used in the determination of gas exchange and functional residual capacity (FRC) in lung function laboratories. Patients receiving ventilatory support at an intensive care unit (ICU), however, in whom gas exchange and related physiological indexes might be of special interest and value, do typically not benefit from all these advanced methods, because

- they are unable to cooperate in diagnostic procedures,
- unlimited, full access to them is required at all times for therapeutic procedures,
- they are in unstable cardiopulmonary condition and are connected to multiple instruments (ventilator, ECG, pacer, catheters, catheter gauges and the like) which render any dislocation difficult and risky.

Under these difficult conditions the choice of methods for gas exchange measurement is virtually reduced to open-system, time resolved gas balancing [15]. No gas is accumulated or collected when using this method; there are no bags, no mixing chambers or special valves, all of which would unacceptably interfere with the numerous and frequent clinical routine procedures. Instead, accumulation is done continuously and computationally as the gas passes a small measuring head which is inserted between the swivel connector of the endotracheal tube and the Y-piece of the respiratory circuit. The measuring head for open-system gas balancing must allow for simultaneous measurement of gas flow and gas composition so the two measurements can be combined to yield realtime balances of individual gases. Only such a minimum hardware solution will provide results that are truly representative of a patient's respiratory status.

Currently, respiratory mass spectrometry provides the most versatile and accurate means of measuring gas composition. Even more importantly, a mass spectrometer provides the signal bandwidth which is required for time resolved gas balancing. A 90% response time of 100 ms for each gas channel is to be regarded as the upper limit for an useful instrument [8]; mass spectrometers reach response times well below this limit. This combination of features distinguishes a mass spectrometer from other instruments which might be cheaper but are either too slow or too inaccurate, or too limited in versatility. Mass spectrometers however are incompatible with clinical routine in most settings; if one is being used, it must be typically operated remotely from the ICU. This necessitates the use of a long transport capillary to convey the gas samples from the measuring head to the mass spectrometer. Moreover, due to the expense of a mass spectrometer, it typically serves as a central analyzer for several ICU beds via valve-switchable capillaries [17].

Figure 1 shows a schematic view of a typical *sidestream* measurement configuration using a mass spectrometer. The gas transport through the capillary is driven by a mechanical vacuum pump inside the mass spectrometer, so the capillary becomes an integral part of the pressure control elements of the inlet system of the mass spectrometer. Therefore the geometry of the capillary must be reasonably selected, and be designed to ensure a stable inlet pressure of the instrument, largely independent of any changes in airway pressure that may be present in the measuring head. This is usually done by selecting a large ratio

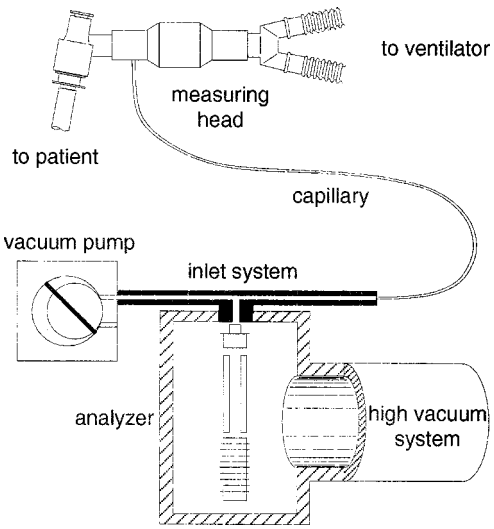

Fig. 1. Schematic of the arrangement for using a respiratory mass spectrometer as a *sidestream* gas analyzer for intubated patients.

of pressures at the entrance of the capillary (at the measuring head), which is approximately atmospheric pressure, and at the exit of the capillary (at the inlet of the instrument). These conditions are typically fulfilled with a capillary which has <1 mm inner diameter and is ≈ 3 m long.

A constant transport delay would not present a problem, since the data acquisition system and computer had only to shift the sequences of measurement results of gas flow and gas composition relative to each other, according to the delay experienced by the gas samples. But in every situation that is of interest in terms of gas exchange and gas balancing, gas composition varies largely with inspiration and expiration, which in turn affects transport delay time due to changes in the viscosity of the gas samples. Gas exchange measurements will respond most sensitively to errors in synchronization at times of major changes in gas composition, for obvious reasons. Moreover, the changes of gas composition occur predominantly at the onset of inspiration and expiration, where, in the case of full mechanical ventilation, the gas flow is maximum in either direction. This will further promote the formation of errors, for false gas compositions are potentially attributed to large proportions of the tidal volume. So it is most important to have continuous information on the varying delay time, irrespectively of specific breath phases. The algorithm described here is capable of providing this information, be it in near real time or on data sets that have already been recorded.

The algorithm depends on two basic requirements. First, all major gas components must be measured simultaneously by mass spectrometry. Second, all signals of the mass spectrometer and of the gas flow sensor must be regularly and synchronously sampled and digitized at a rate that allows for breath-by-breath analysis, e.g., 60 Hz.

A third, but not basic, requirement is that a reference signal be recorded in the form of CO_2 concentration measured simultaneously and in real time. This reference signal is to be recorded using a fast mainstream infrared CO_2 sensor operated simultaneously with the mass spectrometer. This additional CO_2 sensor is not specifically needed for the algorithm to be presented here, but it is helpful in combination with every *sidestream* measurement for verifying the correct synchronization of the mass spectrometer signals. Here we use it to show the correct function of the algorithm.

Following a detailed description of the algorithm, we will illustrate its function in the example of an FRC measurement in a patient under mechanical ventilation during recovery from cardiac surgery. FRC determination is in this case done by nitrogen washout using argon as a replacement. The high viscosity of argon leads to sizable changes in delay time which enhances the visibility of the effect.

2. Method

2.1. Technological considerations for the algorithm

The delay of the mass spectrometer signals is caused by the viscous flow of gas samples through the capillary. At the entrance of the capillary, in the measuring head, the pressure is nearly atmospheric while it is held at roughly 1 mbar at the exit. The transport thus involves a decompression by a factor of approximately 1000. A flow of 0.5 ml/s ATP (Ambient Temperature and Pressure conditions) and a capillary diameter of 0.3 mm results in an average velocity of 5 m/s approx. at the entrance, which accelerates up to speed of sound at the exit. The acceleration occurs gradually during the passage, which is associated with a variable pressure gradient along the capillary. It is to be expected that the flow is laminar over the most part of the capillary, with a Reynolds number around 100 near the entrance. The situation towards the low pressure exit is not easily described mathematically, because there exists a

region where the flow regime changes from laminar to a completely different transsonic flow. On the other side, the transit time of gas samples in this narrow region is very short, so errors in mathematical modelling are not expected to produce substantial errors in the calculation of total delay time. Thus we assume laminar flow throughout the capillary for calculation.

2.2. Derivation of stationary compressible gas flow in the capillary

First we will derive the distribution of pressure and velocity (which means the average velocity of laminar flow in the following formalism), in the case of a one-dimensional stationary tubular flow of a uniform gas mixture, as described by Cramers et al. [9]. The differential form of the Hagen–Poiseuille law gives a formula of the volume flow as a function of the pressure gradient:

$$\dot{V}(x) = -\frac{\mathrm{d}p}{\mathrm{d}x} \cdot \frac{\pi r^4}{8\eta}. \tag{1}$$

$\dot{V}(x)$ is the volume flow (at location x), $\mathrm{d}p/\mathrm{d}x$ is the pressure gradient, r is the inner radius of the capillary, and η is the dynamic viscosity of the gas. The flow is considered isothermal since it is in close thermal contact with ambient air through the thin wall of the tubing. In this case pressure is proportional to particle number density n. Due to the gas flow being continuous, the mass transfer $\dot{M}$ is constant throughout the capillary:

$$\dot{M} \propto n\dot{V}(x) \propto p\dot{V}(x) = \text{const}. \tag{2}$$

This implies that volume flow is inversely proportional to pressure. Elimination of $\dot{V}(x)$ from Eqs (1) and (2) yields a differential equation for the pressure profile along the capillary:

$$p\dot{V}(x) = p_1\dot{V}_1 = -p\frac{\mathrm{d}p}{\mathrm{d}x}\frac{\pi r^4}{8\eta} = \text{const}. \tag{3}$$

p_1 is the pressure at the entrance, i.e., the airway pressure in the measuring head, $\dot{V}_1$ is the volume flow at the entrance, and x is the location, measured from the entrance of the capillary. For integration we collect all constant terms:

$$\int p\,\mathrm{d}p = \text{const} \cdot \int \mathrm{d}x \tag{4}$$

and get

$$p^2(x) - p_1^2 = \text{const} \cdot x. \tag{5}$$

The boundary condition at the exit of the capillary of length L, $p|_{x=L} = p_2$, yields

$$\text{const} = \frac{p_2^2 - p_1^2}{L}. \tag{6}$$

Thus, using Eqs (5) and (6), the pressure along the capillary can be expressed as

$$p(x) = p_1 \cdot \sqrt{1 - \beta \cdot \frac{x}{L}} \tag{7}$$

with the abbreviation

$$\beta = \frac{R_\mathrm{p}^2 - 1}{R_\mathrm{p}^2}. \tag{8}$$

R_p is the ratio of pressures at the entrance and exit of the capillary:

$$R_\mathrm{p} = \frac{p_1}{p_2}. \tag{9}$$

The entrance pressure p_1 is near atmospheric pressure, whereas p_2, the vacuum pressure established by the mass spectrometer, is approximately 1 mbar. This results in a large R_p, which in turn makes β nearly unity, thus a reasonable estimation of p_2 is sufficient for further calculations. Using the geometrical definition of average velocity $\overline{v}$ for laminar flow,

$$\dot{V} = \pi r^2 \cdot \overline{v} \tag{10}$$

and Eq. (1) we get

$$\overline{v}(x) = -\frac{r^2}{8\eta} \cdot \frac{\mathrm{d}p}{\mathrm{d}x}. \tag{11}$$

Differentiating Eq. (7) and substituting it into Eq. (11) yields

$$\overline{v}(x) = p_1 \cdot \alpha \cdot \frac{1}{\sqrt{1 - \beta x/L}} \tag{12}$$

with the abbreviation

$$\alpha = \beta \cdot \frac{r^2}{16\eta L}. \tag{13}$$

Equation (12) contains the marked nonlinearity of gas velocity in the region of low pressure, where $x \to L$, $\beta \approx 1$. From Eq. (12) we can calculate the delay time theoretically expected:

$$\overline{v}(x) = \frac{\mathrm{d}x}{\mathrm{d}t} = p_1 \cdot \alpha \cdot \frac{1}{\sqrt{1 - \beta x/L}}, \tag{14}$$

and

$$\mathrm{d}x \cdot \sqrt{1 - \beta \frac{x}{L}} = p_1 \cdot \alpha \, \mathrm{d}t \tag{15}$$

and by integration

$$\int_0^L \mathrm{d}x \cdot \sqrt{1-\beta\frac{x}{L}} = p_1 \cdot \alpha \cdot \int_0^{t_{\mathrm{d,th}}} \mathrm{d}t, \tag{16}$$

$$t_{\mathrm{d,th}} = \frac{2L}{3\alpha\beta p_1} \cdot \left(1-(1-\beta)^{3/2}\right). \tag{17}$$

Generally, this calculated value for delay time, $t_{\mathrm{d,th}}$, does not agree with actual measured delay time. This is mainly due to the poorly controlled inner diameter of the capillary material, which is very likely to influence the delay time due to the nonlinear relationship between diameter and flow resistance of a tube. To come to a practical solution for the mathematical compensation of delay time, we use an effective radius of the capillary, r_{eff}, according to the inverse quadratic dependence of the delay time on capillary radius (13):

$$r_{\mathrm{eff}} = r_{\mathrm{geom}} \cdot \sqrt{\frac{t_{\mathrm{d,th}}}{t_{\mathrm{d,meas}}}}. \tag{18}$$

The algorithm to be described operates on this calculated r_{eff}, which will give exactly the measured delay time when substituted into (17). In Eq. (18), r_{geom} is the radius from the specifications of the capillary material, and $t_{\mathrm{d,meas}}$ the delay time measured in the laboratory with room air. There are several methods for measuring delay time of a capillary, which are all described in detail in the literature [2, 3,5–7,14]. The short transit time of pre-decompressed gas samples from the flow-by duct through the molecular leak into the high vacuum analyzer chamber (refer to Fig. 1) is neglected in the formulas.

2.3. Algorithm for nonstationary compressible gas flow in the capillary

Up to now we have equations for a gas flow of constant gas composition. Next we will derive an algorithm that is capable of dealing with rapid changes of gas composition as they occur in ventilated patients and especially during washout maneuvers. To this end we assume the gas flow within the capillary is composed of a string of discrete gas samples; each sample is considered as having a uniform gas composition, and as being interfaced sharply against its neighbor samples. The samples are defined by the fixed sampling rate of of the data acquisition system connected to the mass spectrometer. This principle of function implies that the allocation of each part of the capillary flow to a certain gas sample is only fixed upon its arrival at the mass spectrometer inlet, after it has traveled the whole distance down the capillary. Consequently the processes inside the capillary must be mathematically reproduced in reverse temporal order to calculate delay time, i.e., transit time of each gas sample along its way through the capillary.

Each gas sample is characterized by the position of its boundaries, the pressures at the boundaries, and its composition. Since each boundary is common to two adjacent samples, it is sufficient to take one reading of the condition at each boundary. For each time step the algorithm completes two tasks: first, it calculates pressures at all boundaries from the actual position of the boundaries; second it calculates the displacement of each boundary under the influence of the local pressure distribution. In this way a free space is produced at the exit of the capillary in each time step, since the calculated displacement of the boundaries is directed towards the entrance of the capillary. This free space, in turn, defines the

gas sample entering the simulation in each time step, together with the gas composition measured by the mass spectrometer at that moment. The delay time pertaining to this gas sample is then simply given by the number of simulation steps, i.e., time steps, taken by it to make its full travel through the capillary.

Changes in gas viscosity cause changes in flow resistance of the capillary, which in turn account for changes in delay time. This mechanism is incorporated in the algorithm as it records the viscosity of each sample. The viscosity η_{wet} of gas samples containing water vapor is approximated by the following empirical formulas [4] from the partial pressures of the constituents:

$$\eta_{\text{wet}} = H_{\text{r}} \cdot \frac{p_{\text{H}_2\text{O}}}{p_{\text{Baro}}} \cdot (-5.55 + 0.35 T_{\text{amb}}) + \eta_{\text{dry}} \cdot \left(1 - H_{\text{r}} \cdot \frac{p_{\text{H}_2\text{O}}}{p_{\text{Baro}}}\right) \tag{19}$$

with η_{dry} from

$$\begin{aligned}\eta_{\text{dry}} = {} & F_{\text{N}_2} \cdot (50.55 + 0.423 T_{\text{amb}}) + F_{\text{CO}_2} \cdot (11.20 + 0.461 T_{\text{amb}}) \\ & + F_{\text{O}_2} \cdot (49.60 + 0.521 T_{\text{amb}}) + F_{\text{Ar}} \cdot (34.95 + 0.635 T_{\text{amb}})\end{aligned} \tag{20}$$

and $p_{\text{H}_2\text{O}}$ from

$$p_{\text{H}_2\text{O}} = 13.2 - 0.61(T_{\text{amb}} - 273) + 0.04(T_{\text{amb}} - 273)^2. \tag{21}$$

η_{wet} and η_{dry} are dynamic viscosities in μ Poise, T_{amb} is ambient Kelvin temperature, H_{r} is relative humidity, and p_{Baro} is barometric pressure.

The above formulas are based on three major assumptions. First it is assumed that N_2, CO_2, O_2, Ar, and H_2O constitute all major components of the gas being breathed. If additional test or tracer gases are being used, they must be accounted for in the above formulas using appropriate coefficients. Second it is assumed that the viscosity of each constituent depends linearly on temperature. More accurate estimations have been derived, e.g., by Keyes [13], but the small temperature range covered in respiratory measurements allows for this simplification. Third, the viscosity of the gas mixture is taken to be a weighted average of the viscosities of the pure constituents. This assumption can be made in the present case with only nitrogen, oxygen, carbon dioxide, and argon as components of the gas mixture. Different approximations must however be used if helium is present, for it causes a nonlinear dependence of viscosity of the mixture on helium concentration [12].

The mass spectrometer is adjusted to measure the four gas concentrations as fractions of the dry component of the gas mixture. The water vapor concentration of the gas mixture is not measured for practical difficulty. Instead, $p_{\text{H}_2\text{O}}$ is calculated from ambient temperature and an assumed relative humidity H_{r} of 0.6. Formula (21) [4] approximates standard data, as given, e.g., by Alexandrov [1]. Gas viscosity is nearly independent of pressure in the range between atmospheric and coarse vacuum, thus the algorithm uses a fixed viscosity per gas sample.

2.3.1. 1st part of the algorithm: calculation of pressure distribution

To integrate the differential Eq. (3), all constant terms were collapsed thus producing the simple expression (4) for the determination of pressure distribution. Now we include the nonuniformity of viscosity $\eta(x)$. Based on Eq. (3), the integral equation corresponding to (4) is

$$\int p \, \mathrm{d}p = \text{const} \cdot \int \eta(x) \, \mathrm{d}x \tag{22}$$

and

$$p^2(x) - p_1^2 = \text{const} \cdot \int_0^x \eta(\xi)\,\mathrm{d}\xi. \tag{23}$$

The boundary condition at the exit of the capillary of length L, $p|_{x=L} = p_2$, gives, in analogy to Eq. (6), a value for const of

$$\text{const} = \frac{p_2^2 - p_1^2}{\int_0^L \eta(\xi)\,\mathrm{d}\xi}. \tag{24}$$

This gives an expression of the pressure distribution $p(x)$ along the capillary,

$$p(x) = p_1 \cdot \sqrt{1 - \frac{\beta \cdot \int_0^x \eta(\xi)\,\mathrm{d}\xi}{\int_0^L \eta(\xi)\,\mathrm{d}\xi}}. \tag{25}$$

At this point we divide the hitherto continuous gas flow into discrete gas samples, which is illustrated in Fig. 2. To this end, Eq. (25) is written in a discrete form as follows:

$$p_{k+1} = p_1 \cdot \sqrt{1 - \beta_D \cdot \sum_{i=1}^{k} \eta_i \cdot l_i} \tag{26}$$

with the abbreviation

$$\beta_D = \frac{R_\mathrm{p}^2 - 1}{R_\mathrm{p}^2 \cdot \sum_{i=1}^{N} \eta_i \cdot l_i}. \tag{27}$$

η_i is the viscosity of the ith sample, l_i is the length of it. R_p is defined in Eq. (9). The capillary contains a total of N samples; they are counted up from the entrance of the capillary. The formulas Eqs (26) and (27) represent the first part of the algorithm; they are used to calculate the pressures at the interfaces between the samples, from a known local distribution of all samples within the capillary.

2.3.2. 2nd part of the algorithm: calculation of displacements

To calculate displacements it would be a straightforward solution to use a discrete form of Eq. (12) which gives average gas velocitiy, and to multiply this with the duration of one time step. Such a linear extrapolation, however, will not work due to the strong nonlinearity of the velocity profile near the exit of the capillary. It would lead to interfaces of adjacent gas samples being displaced such as to produce a crossover of the samples, thereby breaking up the temporal and local sequence of the samples.

Instead we consider each gas sample as a short piece of uniformly filled capillary tubing, and let the pressures present on its two ends, as calculated in the first step, be the inlet and exit pressures of this short capillary. In analogy to Eq. (17), the transit time of the kth sample t_{dk} amounts to

$$t_{dk} = \frac{2l_k}{3\alpha_{dk}\beta_{dk}p_k} \cdot (1 - (1 - \beta_{dk})^{3/2}) \tag{28}$$

with the abbreviations

$$\alpha_{dk} = \frac{\beta_{dk} \cdot r_{\text{eff}}^2}{16\eta_k l_k}, \tag{29}$$

$$\beta_{dk} = \frac{R_{\text{p}k}^2 - 1}{R_{\text{p}k}^2}, \tag{30}$$

$$R_{\text{p}k} = \frac{p_k}{p_{k+1}}, \tag{31}$$

l_k is the length of the kth sample, η_k is gas viscosity calculated using (19), r_{eff} is the capillary radius, p_k and p_{k+1} the pressures acting on the interfaces of the kth sample. The resulting transit time t_{dk} is the time required to move the $(k+1)$st interface exactly back to the location of the kth interface. This differs from the full duration $t_{\text{samp}} = 1/f_{\text{samp}}$ of one time step by

$$\Delta t_k = t_{dk} - t_{\text{samp}}, \tag{32}$$

Δt_k is used to estimate the new location of the kth interface:

$$x_{k,t=-t_{\text{samp}}} = x_{k,t=0} + \Delta x_k, \tag{33}$$

with the displacement Δx_k,

$$\Delta x_k = l_k \cdot \frac{(1 - (1 - 1.5 \cdot \alpha_{dk}\beta_{dk}p_{k+1}\Delta t_k/l_k)^{2/3})}{\beta_{dk}}. \tag{34}$$

The counting variable k is running from 1 to N, starting from the entrance of the capillary. After the displacements are calculated using Eq. (34), the positions of the interfaces are correspondingly corrected using Eq. (33). Then, the gas concentrations of the samples are passed over in the backward direction, i.e., from sample $k+1$ to sample k. This completes the second step of the algorithm and leaves the capillary with all samples displaced by approximately one place to the left (see Fig. 2).

2.3.3. Changes in total delay time

When the algorithm starts calculating Δx_1 at the entrance of the capillary, this quantity usually becomes zero or negative, which then means that the right interface of the first sample, located at x_2, will leave the capillary during the actual time step. In this case, the loss of this one sample is balanced by the intake of one new sample at the exit of the capillary, and the total delay time of the capillary remains unchanged. This is the case if the gas composition is constant, and the gas flow is stationary throughout the capillary.

Occasionally Δx_2 is found to be of sufficiently negative value to cause even the interface located at x_3 to leave the capillary during the actual time step, together with the interface at x_2. In this case, two samples will leave the capillary in a single time step, whereas only one new sample is taken in at the exit of the capillary. So, the total delay time is decreased by one time step in the direction of the simulation, and is consequently increased in the original temporal order. Physically, this represents a rise in viscosity of the gas entering the capillary.

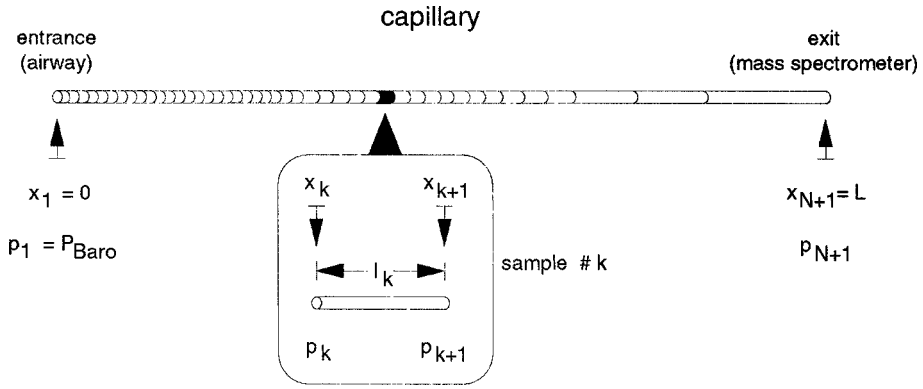

Fig. 2. Schematic of the numbering of gas samples in the capillary used in the algorithm.

Conversely, if Δx_1 is found to be positive, the first sample will not completely leave the capillary in the actual time step but is retained partially, and is cut off at the entrance of the capillary. The total delay time then increases by one time step in the direction of the simulation, and consequently decreases in the original temporal order. In this way the total number of samples can decrease at maximum by one per time step; this represents the physical situation in which a gas with low viscosity is entering the capillary.

2.3.4. Processing complete data files

Alternatingly applying the above two steps, the algorithm simulates the gas flow in equidistant time steps, which correspond to the sampling rate of the data acquisition system. Due to the algorithm working in reverse temporal order, there must be data available before starting the analysis. The simplest solution is to analyze a complete data file in reverse order, but this will completely disable realtime analysis. To regain at least some capability of processing the data in nearly real time, the algorithm was designed to process them in blocks of a certain length. The samples within each block are processed in reverse temporal order as outlined above, whereas successive blocks are processed in original temporal order, as they are read in from a data file or are produced by a data acquisition system.

The problem of continuity between blocks has been solved by letting the algorithm work through a portion of the temporally succeeding block before starting with the actual block of interest. In this way the simulation already produces stable results with a filled capillary as it begins working the actual block. A practically useful block size of 512 samples, and an overlap of 200 samples of the succeeding block for initializing the algorithm have been experimentally determined. One working cycle of the algorithm, therefore, encompasses 712 samples, 512 of them being useful data, and 200 of them being discarded after having served the initialization process.

At the beginning of a working cycle, there is nothing known about the distribution and pressures of the samples along the capillary. The algorithm starts by assuming that the entire capillary is filled uniformly with gas of the composition of the sample #712, the pressures at the entrance and exit being known to be atmospheric pressure and vacuum pressure of the mass spectrometer, respectively. Using Eq. (34), the displacement of the interface directed to the mass spectrometer during one time step ($1/f_{\mathrm{samp}}$) is calculated. This produces a free space at the exit of the capillary, which is then filled uniformly with gas of the composition of the sample #711. This completes the first simulation step and leaves the capillary containing two samples with one interface between them.

The second simulation step starts with (26) to calculate pressures at the central interface, followed again by (34) to calculate the resulting displacements. After this, gas of the composition of the sample

#710 is filled into the free space at the exit of the capillary. This scheme is repeated until the sample #1 is taken into the capillary. The samples are thus moving in reverse order through the capillary, as if the mass spectrometer were producing the samples and pushing them towards the entrance of the capillary.

To actually make the synchronization between gas concentration and gas flow, the useful 512 samples are now rearranged such that the gas concentrations of a sample just leaving the entrance of the capillary are associated with the flow signal being measured coincidentally with the sample just making its transition from the mass spectrometer into the capillary. Finally, the useful 512 sample block is stored back onto mass storage, and #513 through #712 are discarded.

In the following work cycle, the procedure starts with the samples #513 through #1224, this time having #513 to #1024 among the useful samples and discarding #1025 through #1224. In this way the entire data file or data stream is treated in separate blocks, with the overlap providing continuity.

3. Investigation

3.1. Clinical setting

We validated the function of the algorithm using data we recorded in patients at the cardiac surgical intensive care unit who were included in a study involving detailed noninvasive lung function analysis. The study was approved by the ethical commitee of our institution. Of these, we present the data of one patient mechanically ventilated for recovery from open heart procedure. The patient was tracheally intubated and connected to an EV-A ventilator (Drägerwerk AG, Lübeck, Germany). Clinical data are given in Table 1. Inert gas washout was performed to assess functional residual capacity. This was done by replacing the N_2 fraction of inspiratory gas with argon while maintaining the inspiratory O_2 fraction constant.

3.2. Instrumentation

We use an open circuit configuration with a measuring head inserted between the swivel connector of the patient's endotracheal tube and the Y piece of the breathing circuit as shown in Fig. 1. The measuring head consists of a Fleisch type pneumotachometer flanged together with an infrared absorption CO_2 mainstream sensor. The mass spectrometer is equipped with a 3.5 m long capillary of 0.3 mm inner

Table 1
Clinical and respiratory data of the patient after aortic valve replacement. Ventilatory mode was volume controlled CPPV

Age	57 yr
Weight	67 kg
Length	172 cm
FIO_2	0.4
Respiratory frequency	11 min^{-1}
Tidal volume	820 ml
Inspiratory flow	330 ml/s
Expir. minute volume	9.2 l/min
Dead space ventilation[19]	1.1 l/min
End tidal CO_2 conc.	3.3%

diameter. The tip of the capillary was introduced into the measuring head and fixed at a position immediately adjacent to the infrared beam of the mainstream CO_2 sensor, to assure simultaneous measurement of CO_2 concentration *in situ* and suction of corresponding gas samples by the mass spectrometer.

The pneumotachometer is size no. 2, and heated to prevent water condensation. Since the pneumotachometer is influenced by gas viscosity in much the same way as the sampling capillary, we use the synchronized gas concentration signals of the mass spectrometer to correct the flow signal for changing gas composition, as described in [4], using the formulas Eq.(19) through Eq.(21).

The mass spectrometer is a quadrupole type instrument (Centronic 200MGA medical gas analyzer, Pollution & Process Monitoring Ltd., Borough Green, Sevenoaks, Kent, UK). This instrument has eight gas channels, and a response time of 80 ms approx. Four gas channels were tuned to N_2, CO_2, O_2, and Ar. The infrared absorption CO_2 mainstream analyzer is a fast-responding Siemens 930, (Siemens-Elema, Solna, Sweden).

3.3. Quantification of delay error

Error in synchronization was assessed by comparing the two CO_2 signals (mass spectrometer vs. the infrared mainstream sensor) at the moments of steep transition from low to high CO_2 concentration at the start of expiration e.v.v. The transitions through a concentration half way between zero and end tidal concentrations were taken as time markers. This gave two data points per breath.

3.4. Data processing

All signals were sampled at a rate of 60 Hz, digitized 12 bits wide and stored for offline analysis. All corrections were done computationally using the digitized signals. The offline data processing was done on a Sun Microsystems SparcStation 2 running Solaris 2.3, the synchronization algorithm and its graphical working environment were coded and compiled using SPARCworks SPARCompiler C++ version 3.0.1. (SunSoft, SunPro, Sun Microsystems Inc., 2550 Garcia Avenue, Mountain View, CA 94043, USA). The synchronization algorithm was implemented according to the Eqs (26) and (34).

4. Results

Figure 3 shows two breaths at the onset of the washout maneuver. The top tracing shows the instantaneously measured flow versus time. The second tracing shows N_2 fraction from the mass spectrometer, one corrected for a fixed delay time, and the other corrected dynamically using the new algorithm. The third tracing shows the two superimposed CO_2 curves from the Siemens 930 and from the mass spectrometer, the latter synchronized with a fixed delay compensation adjusted for synchronism before the beginning of the maneuver. The fourth tracing shows the same two CO_2 curves, but with the mass spectrometer signals synchronized using the new algorithm. It can be seen that the synchronization becomes erroneous at the onset of the maneuver when a fixed delay compensations is used, whereas it is continuously adapted with the new algorithm.

Figure 4 illustrates the function of the algorithm; it shows a zoomed-in view of the onset of the first inspiration of the washout maneuver. The top and bottom tracings show argon concentration versus time, at the mass spectrometer (exit of the capillary), and at the patient's endotracheal tube (entrance of the capillary), respectively. The middle diagram shows a map of the simulated gas flow in the capillary during this time. The ordinate of this diagram represents position: bottom ($x = 0$) the entrance of the capillary,

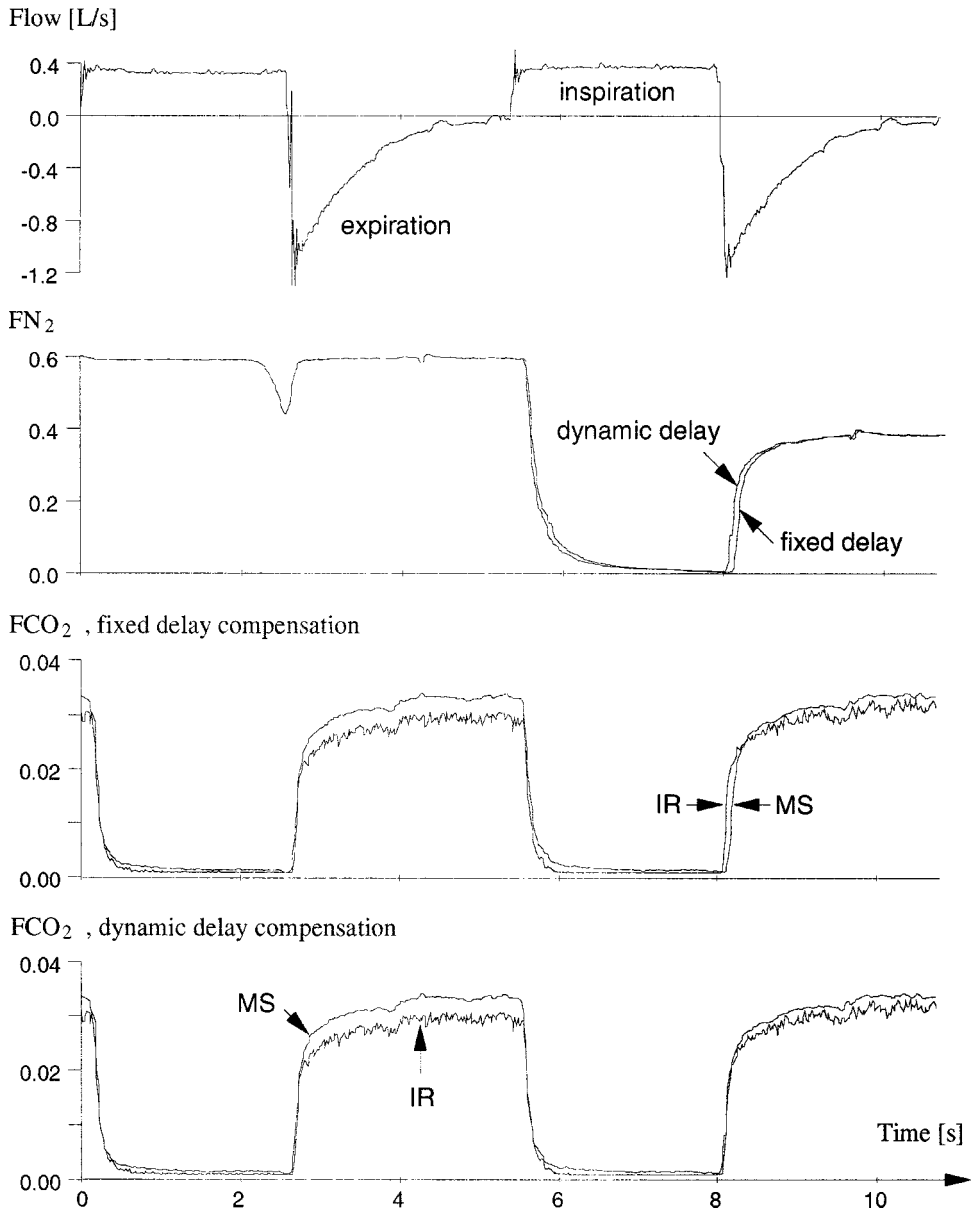

Fig. 3. Flow, N_2, and CO_2 concentration profiles at the start of a nitrogen washout maneuver. Two breaths are shown, the second being the first with N_2-free inspiration. Abbreviations: IR: infrared mainstream CO_2 analyzer Siemens 930; MS: mass spectrometer MGA200.

top ($x = L$), exit. Two sets of curves are shown within. The nearly horizontal curves indicate positions of the interfaces between samples (curves of constant k). The inclined curves indicate the progress of individual samples through the capillary (curves of constant gas composition). The gas concentration measured at a certain time in the top tracing is transferred along the inclined curve that starts at this time, and charted in the bottom tracing at the time where this inclined curve ends. It can be seen in the middle diagram that upon sudden inrush of argon, the delay time gradually increases by approximately five time

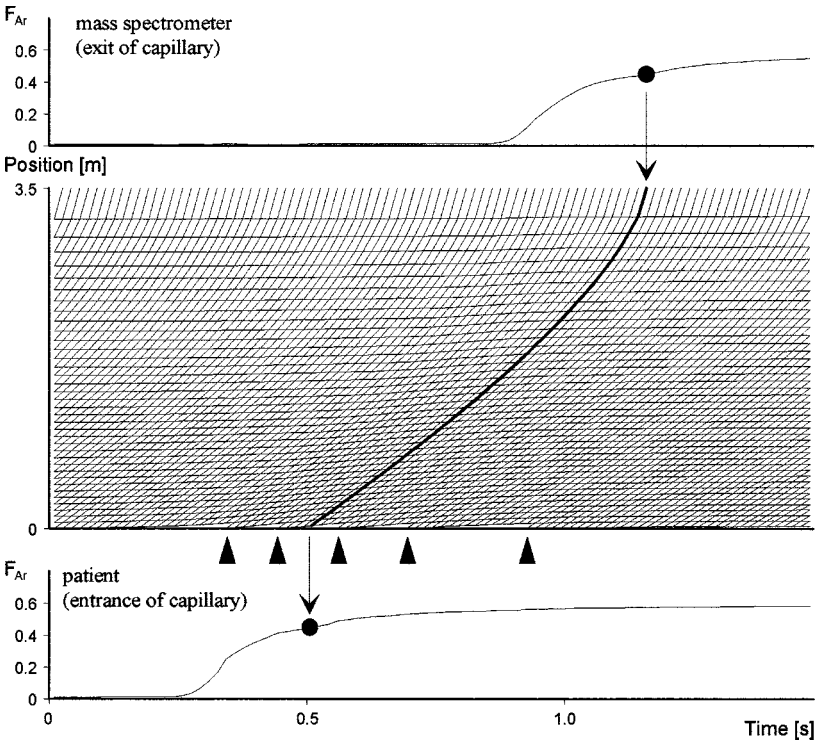

Fig. 4. Argon concentration profiles at the onset of argon washin. Top tracing: reading of the mass spectrometer. Center diagram: map of sample positions versus time. Bottom tracing: resulting reconstructed profile at the patient's airways. The map is the result of the simulation algorithm; with its help the synchronization of concentration profiles is done, as shown with the sample path marked bold. The five arrows point out the moments when the delay time of the capillary increases by one ampling period.

intervals, which means 80 ms at the sampling rate of 60 Hz, and leaves the capillary packed with more and shorter gas samples, compared to the prior situation. This increase extends over 1 second's duration. It is also obvious that the change in delay time causes a distortion of the shape of the rising edge of the concentration curve.

Figure 5 is a diagram of delay error occurring with a fixed delay compensation versus delay compensation with the new algorithm, during the entire washout maneuver, measured through comparison of the two CO_2 signals as described above. Here we see the ability of the algorithm to dynamically correct for changing transport time due to high gas viscosity of argon.

Finally, from the analysis of the washout maneuver shown in Fig. 4, we obtain an FRC estimate of 1315 ml with the new algorithm, whereas it is 1066 ml with a simple fixed delay compensation adjusted for synchrony with normal inspiratory gas mixture. This results in a 19% underestimation without a dynamic correction for changing delay time.

5. Discussion

As a first intuitive result, it is noteworthy that for respiratory gas exchange measurements, the effect of an error in delay time compensation does not cancel out in inspiration and expiration. This can be seen in Fig. 3 in the third tracing for CO_2 elimination. An insufficient delay compensation will result in a delayed

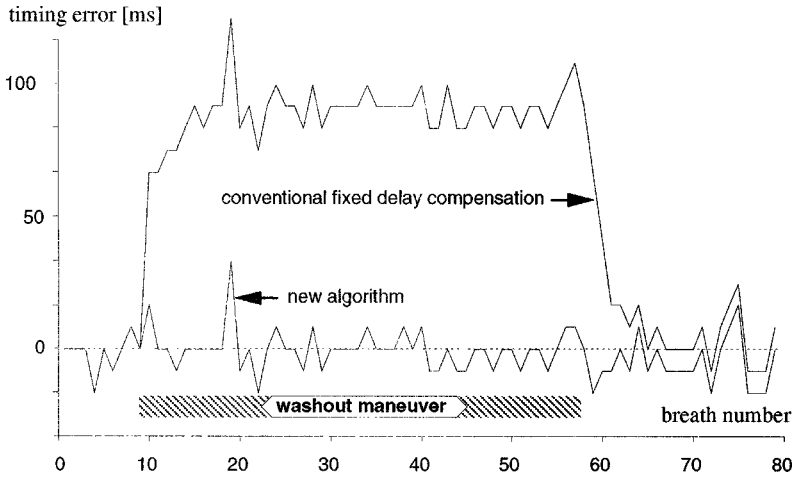

Fig. 5. Delay error observed during a complete nitrogen washout maneuver, including 80 breaths. Each vertex of the curves is the mean value of delay errors detected in CO_2 concentration at the onset of inspiration and expiration. Errors are given in sampling time intervals of 16.6 ms according to 60 Hz sampling rate.

rise of CO_2 concentration in expiration, which means an underestimation of expired CO_2 volume. In inspiration, the delayed fall in CO_2 concentration leads to an overestimation of rebreathed CO_2 volume. Together, both effects will accumulate towards a significant underestimation of CO_2 output. The same applies for N_2 volume balance during the washout maneuver.

In the case of controlled mechanical ventilation, as shown in Fig. 3, an error in delay time will most critically affect gas balances, because the steep changes in gas concentrations occur exactly in those moments when the flow is maximum in either direction. Additionally, it is exactly at these moments that major changes in gas composition will take place, with concomitant changes in delay time due to changes in gas viscosity. Advanced diagnostic techniques and algorithms such as momentum analysis of CO_2 expirograms and gas exchange efficiency analysis [19] essentially depend on reliable timing of the gas concentration profiles. The changes in delay cannot be assumed to occur at defined times, but always come about gradually, depending on the ventilatory pattern and gas composition in use.

The new algorithm does not make any assumptions on all these variables. Another feature of the algorithm is that it does not require that the total delay be typically shorter than the shortest phase of the breathing pattern. A 3.5 m long capillary, as used in the present configuration, delays the gas samples by approximately 700 ms, which would set a lower limit of roughly one second for an inspiration or expiration. This does not mean, however, that there is no upper limit in the length of the capillary, since transversal diffusion [18] and gas adsorption tends to flatten out concentration profiles thereby severely limiting the useful signal bandwidth. Carlon et al. [6] described the practical effect of this limitation in a system with up to 30 m long capillaries.

As illustrated in Fig. 4, the algorithm automatically corrects for distortions experienced by the concentration signals during changes in delay time. This correction, however, is done in finite time increments, according to the sampling frequency; this means that changes in delay time are necessarily realized by either swallowing of information carrying samples, as is the case with the increasing delay time in Fig. 4, or by interposing additional samples without additional information. From this point of view, the transfer of gas samples through the capillary is associated with irreversible loss of data, while the new algorithm is designed to preserve as much as possible of what is observable at the exit of the capillary.

Figure 5 shows that changes in delay of five time intervals, i.e., 80 ms with the 60 Hz sampling rate, are truly compensated by the algorithm, as there is no trend visible in the corresponding curve. We see, however, interspersed fluctuations in delay error, that occur synchronously in both curves. These indicate a limitation that is common to all methods using capillaries, and they originate from fluctuations of the gas flow upon suction of foreign bodies, e.g., secretions from the patient or water droplets as well as particles suctioned from the ambient air. This suggests that an additional filtering device may be required to prevent aspiration of such particles, but then it needs to be designed so as not to introduce additional fluctuations or to release particles of its own.

The FRC measured here is typical of patients under anesthesia and mechanical ventilation, even if it is only of several hours duration. It is massively reduced compared with normally expected values around 3 l in a sitting position. This highlights that there are major and disadvantageous changes in lung parameters soon after initiation of mechanical ventilation. Associated effects have been recognized as early as 1974 by Hewlett et al. [11] and been further investigated by Rehder et al. [16] and Hedenstierna et al. [10] using different techniques. Hedenstierna et al. [10] have shown immediate formation of atelectasis upon induction of anesthesia very clearly by using computed tomography, and concomitant impairment of gas exchange.

There is a clear trend to shortening mechanical ventilatory support, and guiding the patient towards a weaning from it as soon as possible, as prolonged mechanical ventilation has been recognized to slow recovery from pulmonary changes or even to induce new complications. Here the new algorithm can be of use as it is able to noninvasively monitor these changes, which are hard to see from outside, on the spot, with low uncertainty, and with little interference to clinical routine.

The fact that the algorithm cannot be used for true realtime monitoring, as set out above, is not as severe as it appears at first. The FRC estimation, for example, is by itself a multibreath maneuver that requires several minutes to complete, and can then be analyzed as a whole. Furthermore, continuity of the data can be maintained as shown above, by dividing up the original data stream, and processing the stretches in separate runs.

6. Conclusion

We present here an algorithm that compensates for delay time in respiratory mass spectrometry, and for its variations due to changes in gas compositions. It provides a compensation that is based on the physical principles governing the gas transport in the capillary, rather than on gas exchange test results obtained from some specific laboratory setup. We chose this approach because gas exchange measurements depend on numerous factors encountered in computational gas exchange analysis, e.g., breathing pattern, which may obscure the influence of delay variation and lead to occasionally reasonable results by compensation of errors.

The algorithm has been shown to produce well sufficient synchrony between mass spectrometer CO_2 signal and a simultaneously recorded CO_2 signal from a mainstream infrared sensor. Correct synchrony of the other gas signals is then provided by the simultaneous analysis of all gas species in the same mass filter at the same location.

With this, we have shown that it is possible to keep delay errors down to within the range of uncertainty that comes from the finite sampling interval used in breath-by-breath analysis, and from fluctuations of the gas flow within the capillary.

Acknowledgments

This work was supported by the Swiss National Foundation, grants no 3.956-0.85 and 3200-039382.93, by Drägerwerk AG, Lübeck, Germany, and by the Karl Mayer Foundation, Triesen, Liechtenstein.

The Siemens 930 CO_2 analyzer was kindly put to the authors' disposal by Siemens-Elema, Solna, Sweden.

References

[1] A.A. Alexandrov, A.I. Ivanov and A.B. Mateev, eds, *Draft of the Tables of the Dynamic Viscosity of Water and Steam*, Sov. Nat. Comm. on Prop. of Steam, 1974.
[2] R. Arieli and H.D. van Liew, Corrections for the response time and delay of mass spectrometers, *J. Appl. Physiol.* **51**(6) (1981), 1417–1422.
[3] J.H.T. Bates, G.K. Prisk, T.E. Tanner and A.E. McKinnon, Correcting for the dynamic response of a respiratory mass spectrometer, *J. Appl. Physiol.* **55**(3) (1983), 1015–1022.
[4] J.X. Brunner and G. Wolff, *Pulmonary Function Indices in Critical Care Patients*, Springer-Verlag, New York, Berlin, Heidelberg, 1988.
[5] J.X. Brunner, G. Wolff, G. Cumming and H. Langenstein, Accurate measurement of N_2 volumes during N_2 washout requires dynamic adjustment of delay time, *J. Appl. Physiol.* **59**(3) (1985), 1008–1012.
[6] G.C. Carlon, I.C. Kopec, S. Miodownik and R. Cole, Jr., Frequency response of the peripheral sampling sites of a clinical mass spectrometer, *Anesthesiology* **72** (1990), 187–190.
[7] G.C. Carlon, S. Miodownik, C. Ray, Jr. and I.C. Kopec, An automated mechanism for protection of mass spectrometer sampling tubing, *J. Clin. Monit.* **4** (1988), 264–266.
[8] J.B. Cooper, J.H. Edmondson, D.M. Joseph and R.S. Newbower, Piezoelectric sorption anesthetic sensor, *IEEE Trans. Biomed. Eng.* **28** (1981), 459–466.
[9] C.A. Cramers, P.A. Leclercq, J.G. Lerou and H.H. Beneken, Mass spectrometry in monitoring anaesthetic gas mixtures using long sampling tubes: band broadening in capillary tubes caused by flow and diffusion, in: *Mass Spectrometry in Anaesthesiology*, Vickers and Crul, eds, Springer-Verlag, New York, Berlin, Heidelberg, 1981.
[10] G. Hedenstierna, L. Tokics, A. Strandberg, H. Lundquist and B. Brismar, Correlation of gas exchange impairment to development of atelectasis during anaesthesia and muscle paralysis, *Acta Anaesth. Scand.* **30** (1985), 183–191.
[11] A.M. Hewlett, G.H. Hulands, J.F. Nunn and J.S. Milledge, Functional residual capacity during anaesthesia III: Artificial ventilation, *Brit. J. Anaesth.* **46** (1974), 495–503.
[12] J.O. Hirschfelder, C.E. Curtiss and B. Bird, *Molecular Theory of Gases and Liquids*, J. Wiley & Sons Inc., New York, 1954.
[13] F.G. Keyes, Project SQUID: the heat conductivity, viscosity, specific heat and Prandtl numbers for thirteen gases, Technical report 37, MIT, 1952.
[14] H. Noguchi, Y. Ogushi, I. Yoshiya, N. Itakura and H. Yamabayashi, Breath-by-breath $\dot{V}_{CO_2}$ and $\dot{V}_{O_2}$ require compensation for transport delay and dynamic response, *J. Appl. Physiol.* **52**(1) (1982), 79–84.
[15] J.J. Osborn, S.E. Elliott, F.J. Segger and F. Gerbode, Continuous measurement of lung mechanics and gas exchange in the critically ill, *Med. Res. Eng.* **19** (1969), 19–23.
[16] K. Rehder, A.D. Sessler and J.R. Rodarte, Regional intrapulmonary gas distribution in awake and anesthetized-paralyzed man, *J. Appl. Physiol.* **42**(3) (1977), 391–402.
[17] M.J. Roberts, M.L. Boustred and C.J. Hinds, A multipatient mass spectrometer based system for the measurement of metabolic gas exchange in artificially ventilated intensive care patients, *Int. Care Med.* **9** (1983), 339–343.
[18] G. Taylor, Dispersion of soluble matter in solvent flowing slowly through a tube, in: *Proceedings of the Royal Society, Series A*, Royal Society, London, 1953.
[19] G. Wolff, J.X. Brunner, W. Weibel and C.L. Bowes, Alveolar efficiency for CO_2 elimination and series dead space volume; both are affected by the ventilatory pattern, *Appl. Cardiopulm. Pathophysiol.* **2** (1989), 309–314.